MICROSTRUCTURAL AND THERMAL PROPERTY CHANGES OF CASTABLES AFTER CORROSION WITH BLAST FURNACE SLAG AT DIFFERENT CONDITIONS

Thorsten Tonnesen[1], Lise Loison[1], Rainer Telle[1], Felix Baas[2], Felix Firsbach[2], Dieter Georg Senk[2]
[1]RWTH Aachen University, Institute of Mineral Engineering, Aachen, Germany
[2]RWTH Aachen University, Institute of Ferrous Metallurgy, Aachen, Germany

ABSTRACT

Slags from iron and steel production are important byproduct, which can be processed to be used for instance in road construction or as fertilizer in agriculture. For application in the production of cement, amorphous solidified blast furnace slag is used, also referred to as slag sand. The blast furnace slag exhibits a tapping temperature up to 1700°C, however this stored thermal energy cannot be retrieved yet. In order to develop industrial facility for the heat recovery, the selection of corrosion resistant refractory materials is crucial.

Different refractory bricks and castable materials were tested in contact of molten blast furnace slag in order to describe the mechanisms of corrosion and their suitability for the application process. The first material was an oxide refractory composed mainly of Andalusite, while the second one was SiC based. A thermodynamic model, by using the software package FactSage, was worked out and applied on the different refractory and slag compositions to predict phase formation and corrosion. The microstructural properties of the brick and monolithic samples were characterized after firing by means of porosimetry and Scanning Electron Microscopy (SEM) examinations. Dynamic corrosion tests have been performed on the refractory materials, in particular finger test methodology as described in the European standard (DIN 15418). Dissolution and erosion behavior have been examined. Subsequent to the macroscopic evaluation performed on the infiltrated samples, microscopic characterization and structural changes of the corroded microstructure have been carried out with SEM/EDS and XRD.

The SiC based refractory product was strongly infiltrated, while the high alumina specimen exhibited a high resistance against the molten slag. The microstructural analyse of the high alumina sample revealed the dissolution of the matrix in the blast furnace slag, however with slower kinetics than the SiC based sample. The corrosion experiments were applied on the matrix materials (cements, calcium aluminates, SiC fines) as well as on grog aggegates and full castable mixes. Finally the impregnation and the microstructural change are discussed in regard of changing thermal properties such as expansion, permeability and strength.

Key words: Blast furnace trough, slag, dynamic corrosion test, Andalusite, Al_2O_3-SiO_2-SiC-C

INTRODUCTION

Slags originating from iron- and steel production are nowadays important by-products and undergo a further treatment in a particular technology of the primary process.

The secondary use of such slags leads from road construction to fertilizer and cement production. For the cement production glassy precipitated blast furnace slag is commonly used. The produced amount of slag lies at 25% of the produced pig iron amount and reveals a temperature of 1700°C. Therefore recovery processes for the stored heating energy are observed, granulators with including heat recovery are in focus. For these studies suitable refractory lining parts of slag runners are considered. Carbon as well as SiC play an important role in the corrosion of refractories for blast furnace trough application. But also other oxide compounds such as Al_2O_3, SiO_2 and CaO have to be considered in regard of matrix dissolution and grain segregation [1-3].

EXPERIMENTAL

Refractory materials

A model high alumina castable (96% Al_2O_3) has been used for a first corrosion test set up by means of hot stage microscopy to generate an interface and to observe the infiltration behaviour of refractory castable by the molten slag. Furthermore this was an indication for a reference refractory material with less silica

For the dynamic corrosion trials the refractory materials were distinguished according to their main chemical origins. An andalusite brick material was used on one hand to represent alumina-silicate material. On the other hand an Al_2O_3-SiC-C castable was chosen to focus this state of the art refractory for this application. The chemical analysis of the main components and the mineral composition are given in table 1.

Tab. 1: Composition of the refractory test materials

Component	Type	Andalusite brick	Al_2O_3-SiO_2-SiC-C castable
Al_2O_3	[wt.-%]	63	47
SiO_2		35	11
Fe_2O_3		0,9	1,0
CaO		<<	1,2
TiO_2		0,5	<<
SiC		-	31
C		-	6,0
Andalusite	$Al_2O_3 \cdot SiO_2$	+++	-
Mullite	$3Al_2O_3 \cdot 2SiO_2$	++	+
Corundum	Al_2O_3	+	+++
Quartz	SiO_2	+	+
Cristobalite	SiO_2	-	+
Tridymite	SiO_2	-	+
Moissanite	SiC	-	+++
Baddeleyite	ZrO_2	-	+

Physical property testing

The following physical properties were examined:

- Bulk density and open porosity according to DIN EN 993-1

Wettability testing

The melting, wettability and infiltration behaviour was tested with a hot stage microscope type Leitz Wetzlar/Germany according to standard DIN 51730. The BF slag sample was milled to a grain size <63 µm and hand pressed (1.5 N/mm²) to a cylindrical shape with the dimension of 3 mm height and 3 mm diameter. The test was performed with a heating rate of 10 K/min. at air.

Thermodynamic calculations

Thermodynamic calculations were performed using FACT-Sage^{TM} computation package where particular attention to the form of the temperature dependant descriptions of the thermodynamic parameters and to the compatibility of the solution and substance databases is paid [4].

The calculations used in these studies consider a temperature of 1550°C, the phase assemblage of refractory phases with increasing amount of slag and the residual change of the slag composition due to the solution of refractory oxides [5].

Corrosion testing set-up and procedure

An industrial blast furnace slag was provided. The chemical composition of this slag was analyzed by wet chemistry analyses, the results are given in table 2. The corrosion experiments were performed using a set-up of a rod (finger) test (Fig. 1). In contrast to the static crucible test, dynamic convective forces are also active and enhance further corrosion. Erosive influences can be examined as well. For the rod test a prismatic refractory sample of the size 200x40x40 mm³ is fixed to a specimen holder and is dipped into a crucible containing the molten slag. A graphite crucible with a height of 270 mm and a diameter of 90 mm is used to melt the slag in an induction furnace type Junker MF50. The rotation speed for these corrosion tests was set to 32 rpm, testing temperature was 1550°C for a testing time of 15 minutes. To examine microstructural changes after the corrosion tests polished cross sections of the refractory bars were and analyzed by means of SEM/EDS.

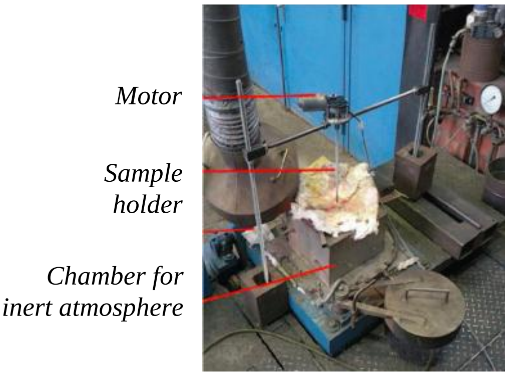

Fig. 1: Finger test set-up with graphite crucible and induction furnace

Tab. 2: Composition of the initial blast furnace slag

Oxide/Component [Wt.-%]	BF slag
SiO_2	34,81
Al_2O_3	13,75
Fe_2O_3	4,45
CaO	38,47
MgO	6,26
TiO_2	1,44
SO_3	0,31
C	0,2

RESULTS AND DISCUSSION

Melting behaviour of the slag: The analyses of the melting behaviour of the BF slag by means of hot stage microscopy revealed the following typical temperatures (fig.2).
Semi-spherical: 1315°C
Flowing temperature: 1342°C

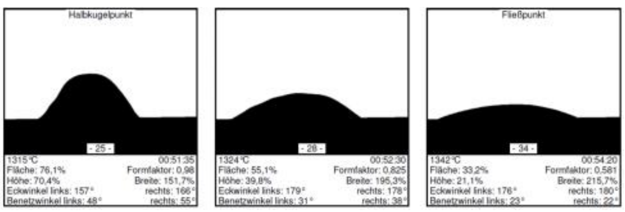

Fig. 2: Melting behavior of the BF slag at air

To generate an interface hot stage microscopy at 1400°C has been performed also with a high alumina castable. The infiltration and reaction behaviour of the slag and the cement bonding is obvious in the micrograph of fig. 3. The grog alumina grains of this 96% Al_2O_3 containing castable are less affected. Small rims of CA phase has been precipitated at the interface between reacted matrix and grog aggregate. EDS of the matrix areas show that the lime-silica rich melt has affected the matrix up to a depth of 15 mm with CA_6 phase formation and small amounts of silica (1.1%). In areas closer to the hot face 12-15% SiO_2 is obvious whereas the lime content differs between 16% and 24%. Na_2O content of 2% and Fe_2O_3 amounts up to 2.7% have been analysed.

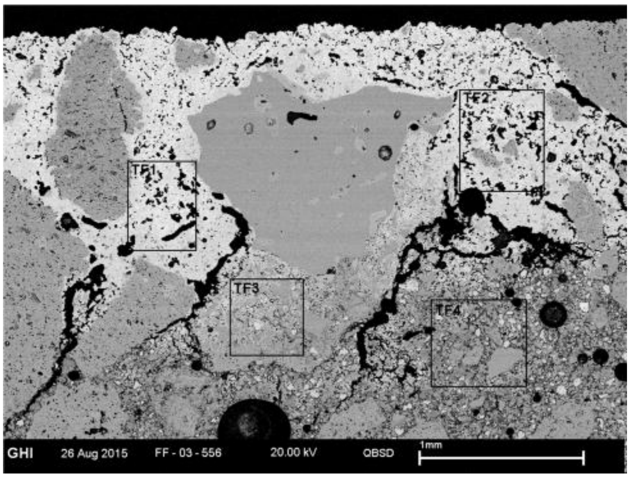

Fig. 3: SEM micrograph: High alumina castable after contact reaction with BF slag at 1400°C

Thermodynamic calculations: The results of the thermodynamic calculations of the two refractory materials in contact with the BF slag at 1550°C are given in fig. 4 and fig. 5. For the andalusite brick composition the decrease of mullite phase and the analogous increase of liquid phase after the initial contact of solid and slag becomes evident (fig. 4 left). With approx. 25% slag amount mullite disintegrates totally and alumina is precipitating. Respectively can be seen the high solubility of silica and alumina in the slag whereas we have a decrease in solubility of lime. FeO is solved in constant amounts (fig. 4 right).
The composition of Al_2O_3-SiO_2-SiC-C shows less liquid formation (fig. 5 left). The dissolution of mullite occurs already at lower slag amounts than for the andalusite. With higher amounts of slag the alumina content gets constantly lower. The decrease of SiC, occuring by oxidation, is also a constant process. The carbon content is stable. In fig. 5 right the solubility of the oxide species is dominantly increasing for alumina. With the total oxidation of SiC and precipitation of SiO_2 the solubility of this refractory species in the slag further increases.

Technological properties of the refractories: The different refractories for the corrosion tests were examined according to their bulk density and apparent porosity. The andalusite brick has a bulk density of 2.64 g/cm³ and an apparent porosity of 12%. The Al_2O_3-SiO_2-SiC-C castable offers 2.56 g/cm³ and 17% apparent porosity respectively.

Corrosion behaviour of andalusite based material: The initial as received microstructure of the andalusite brick is given in fig. 6. The survey documents the loose interconnection of grog grains and matrix revealing gaps and cumulation of larger pores. The brighter matrix consists of mullite with amounts of Fe_2O_3 and TiO_2 contents originating from impurities of up to 300 µm grain size. Cristobalite grains as well as a glassy phase with a silica content of 70%, alkaline oxides of 4.5% and Fe_2O_3 of 1.7% are located in the porous matrix phase.
SEM micrographs of the corroded sample after the finger test with BF slag at 1550°C are given in fig. 7-9.

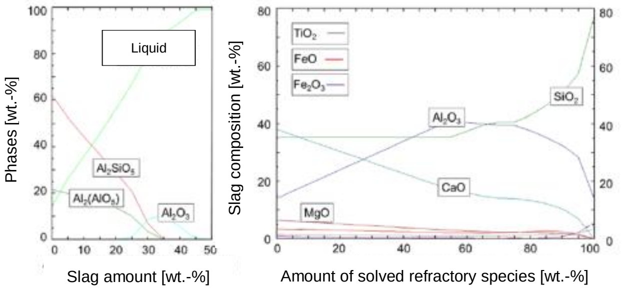

Fig. 4: Thermodynamic calculation: Andalusite brick and BF slag at 1550°C [5]

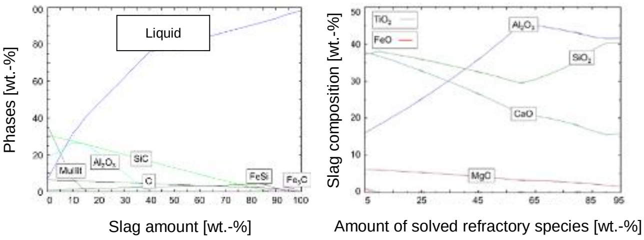

Fig. 5: Thermodynamic calculation: Al_2O_3-SiO_2-SiC-C castable and BF slag at 1550°C [5]

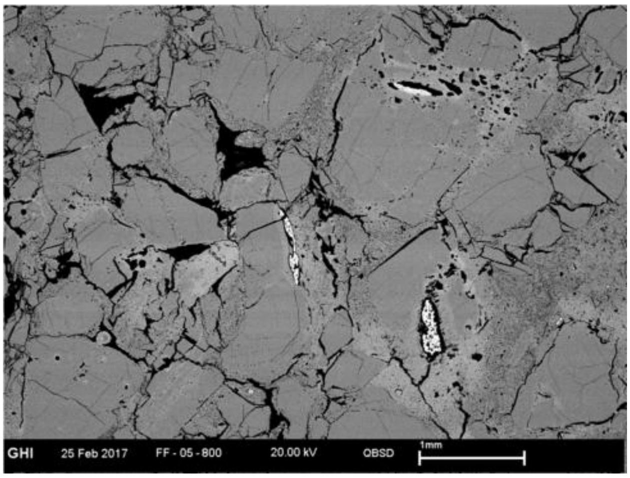

Fig. 6: SEM micrograph: Andalusite brick as received

The survey of the hot face shows an adjacent slag layer of 1 mm dimension and a reaction zone of the porous matrix of further 1 mm (fig. 7). The composition of the adjacent slag identifies with the initial analyses of the slag before. The reaction of the matrix is obvious in fig. 8. On one hand the rims of the mullite grains react with the lime-silica slag. In fig. 8 the rim reveals a mullite structure with 2.5% CaO and 1.7% TiO_2 (Fig. 8 [1]). The infiltrated slag is enriched in silica (45%), lime (9%) and titania (6%) (Fig. 8 [2]). The dissolution of the mullite grains and matrix is in good agreement with the thermodynamic calculations. The initial matrix microstructure apart the reaction zone is unaffected and has the initial bonding phase composition (fig. 8 right porous area).

Corrosion behaviour of Al_2O_3-SiO_2-SiC-C castable: The complex castable microstructure is given in fig. 9. The microstructure consists of grog Al_2O_3-ZrO_2-SiO_2 (AZS) grains in mm-scale. Furthermore dense SiC-, mullite-, alumina- and zirconia-grains are part of the grog fractions. The grains are embedded in a microporous cement matrix with carbon additives.

The progressive corrosion, refractory dissolution and further matrix penetration are remarkable for this castable (fig. 10). Isolated refractory grains are residually spread in a molten slag phase. Nevertheless residual alumina-, AZS- and SiC-grains are

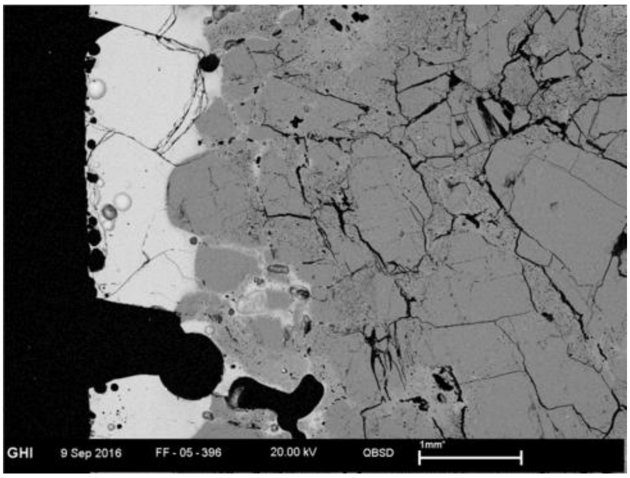

Fig. 7: SEM micrograph: Andalusite brick after corrosion test with BF slag at 1550°C, hot face and adjacent slag

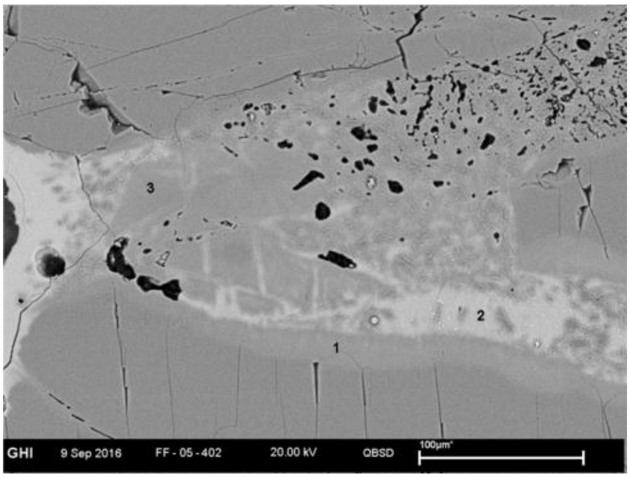

Fig. 8: SEM micrograph: Andalusite brick after corrosion test with BF slag at 1550°C, interface slag – refractory matrix

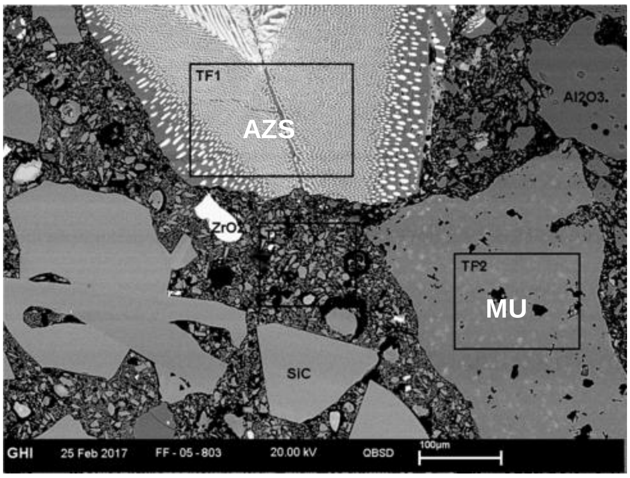

Fig. 9: SEM micrograph: Al_2O_3-SiO_2-SiC-C castable as received

evident although the initial bonding is dissolved (fig. 11). Around the grogs a liquid and after cooling densified matrix zone has been precipitated. It consists of 80% silica, 14% alumina, 2% zirconia and 2% of lime. This shows the high solubility of the matrix constituents in the BF slag. Although for the SiC fines oxidation occurs residual SiC grains could be observed in the fine grained matrix. The interface between slag infiltration and residual refractory microstructure is given in fig. 12. EDS analyses reveal a composition close to the original microstructure. Furthermore in this detail the mechanism of SiC oxidation combined with an ongoing dissolution of the formed silica phases at the hot face becomes evident. Densified slag rich part is locally close to the initial porosity.

CONCLUSIONS

The corrosion mechanisms were studied with two different approaches. The hot stage microscopy with a high alumina castable showed that a temperature with 1400°C approximately 50K above melting temperature does not affect the reaction behavior seriously. Due to a lack of silica CA_6 rims are precipitating at the edges of the grains. In general CA_6 reveals a high viscosity leading to an indirect dissolution behavior of the alumina grain respectively.

The corrosion experiments at 1550°C with the dynamic corrosion test set up result in corrosion mechanisms affecting the microstructure more significant. The andalusite brick was not affected in the same way than the Al_2O_3-SiO_2-SiC-C-castable. A slag layer of the initial slag composition is adjacent at the hot face and just small matrix infiltration and transformation could be observed. Remarkable is the small influence of iron oxide of the slag. Only small matrix areas are penetrated by the lime-silica slag. Due to a stable refractory mullite phase, mainly generated by wet sintering processes, the dissolution is minimized. Even when the interconnection of the grog grains and the matrix is not so strong for the andalusite brick, due to small infiltration the main thermal properties such as expansion and strength will be not affected negatively. Also segregation of grains and severe erosion could not be examined.

In contrast the Al_2O_3-SiO_2-SiC-C-castable showed a high penetration. Due to oxidation processes of SiC grains infiltration and subsequent dissolution of refractory oxides such as alumina and zirconia are the consequence. Since infiltration and the dissolution are dominant the matrix densifies and loss of high temperature performance of the castable will follow. According to the composition high attention is paid on the matrix with SiC and carbon. Oxidation is a major corrosion process for this material. The formation of silicates and other oxides leads to low melting phases densifying the matrix.

Regarding the stability of mullite in the thermodynamic calculations the given corrosion results of the experiments highlight this differently. For the andalusite composition the mullite dissolution in the slag is lowered in contrast to the Al_2O_3-SiO_2-SiC-C-castable. In parallel the amount of alumina in the slag increases for the Al_2O_3-SiO_2-SiC-C-castable. Both can be recognized in the matrix phase formation after the corrosion experiments.

REFERENCES

[1] Camelli S., Plá G., Marinelli P., Doro E., Mirabelli J., Lalla N., Analsis of the Wear Mechanism of Al_2O_3-SiC-C Blast Furnace Runners, Proc. 6th. IAS Ironmaking Conference 2007, Rosario, Argentina, p. 471-478

[2] Prompt N., Ouedraogo E., High Temperature Mechanical Characterisation of an Alumina Refractory Concrete for Blast Furnace Main Trough, J. Euop. Cer. Soc. 28, 2008, p. 2859-2865

[3] Lee W.E., Chan C. F., Microstructures and Slag Resistance of Al_2O_3-SiO_2-SiC-C, Proc. UNITECR, 1997, p. 1593-1602

[4] Bale C. W., Pelton A. D., Thompson W. T.: FACT-Sage - User's Manual. Ecole Polytechnique de Montréal

[5] Baas F., Master thesis RWTH Aachen University, Institute of Ferrous Metallurgy 2016

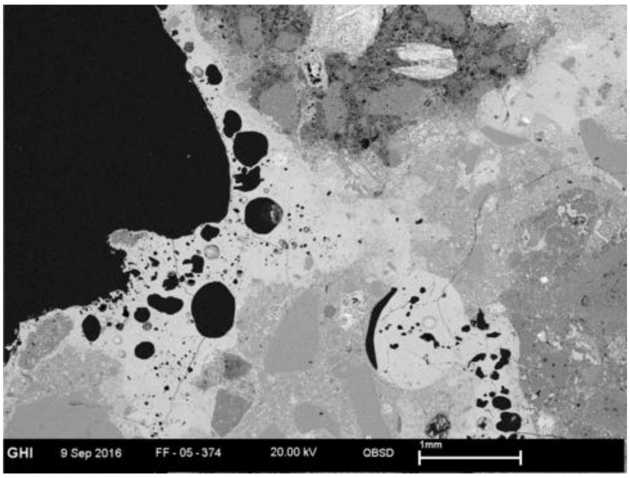

Fig. 10: SEM micrograph: Al_2O_3-SiO_2-SiC-C: Hot face

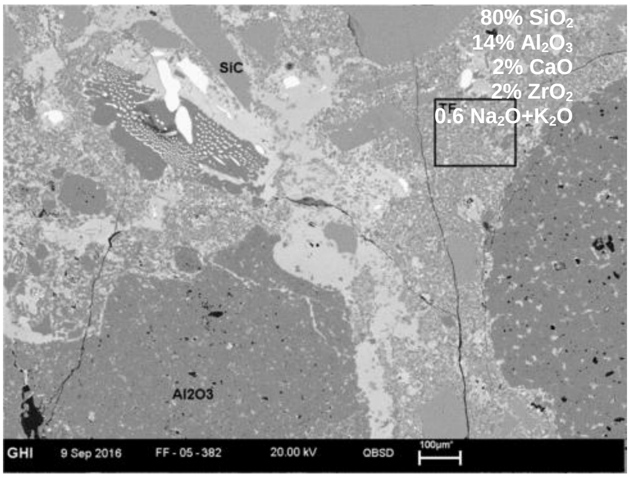

Fig. 11: SEM micrograph: Al_2O_3-SiO_2-SiC-C: Oxidation of SiC and dissolution of the matrix

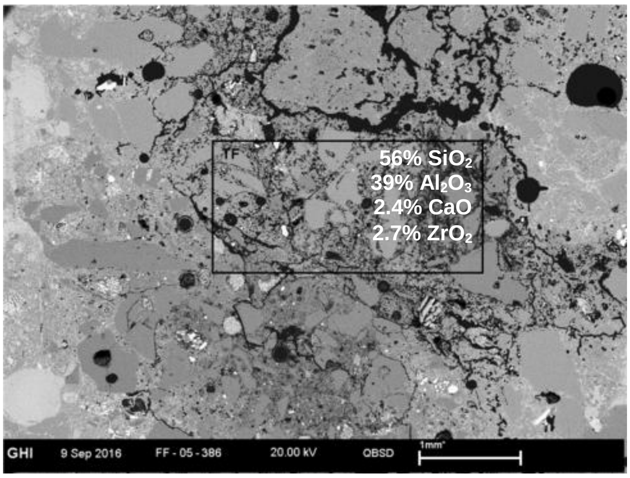

Fig. 12: SEM micrograph: Al_2O_3-SiO_2-SiC-C: Interface of corroded area and residual bulk refractory material